Journal of the Korean Society of Oceanography
Vol. 33, No. 3, pp. 53—63, September 1998

Simulation of Sea Water Response in Deukryang Bay to Typhoon Using the Princeton Ocean Model

CHUL-HOON HONG
Research Center for Ocean Industrial Development, Pukyong National University, Pusan 608-737, Korea

The Princeton ocean model (POM) with free surface in sigma-coordinate, governed by primitive equations, is used to examine the response of sea water in Deukryang Bay to a typhoon. The model reproduces reasonably well the main features in the wind-driven dynamics due to passing of a typhoon. In response to the wind, the coastal jet develops and the upwelling (or downwelling) occurs dominantly in both sides of the bay. This result implies that there should be an overturn in the bay water with the passing of typhoons. Numerical results of POM are also compared to those of a depth-averaged model. From the comparison, it is postulated that the bottom drag coefficient conventionally used for the two-dimensional flow models is inadequate due to overestimation of the computed current field.

INTRODUCTION

Due to basically barotropic response of the ocean to a typhoon, storm surges have been studied in terms of depth-averaged, two-dimensional (2D) models (Platzman, 1963; Heap, 1969; Konish, 1989; Oh and Kim, 1990). In the 2D model, however, it is likely to underestimate not only current fields but also the sea surface elevations since the effect of storm surges is mainly confined to the surface layer of several hundred meters deep.

Hearn and Holloway (1990) compared the amplitudes of elevation of storm surges in the coastal areas between 2D and three-dimensional (3D), barotropic multi-level models, and concluded that there is a discrepancy of about 30% between the elevation in the 2D model and the observation, whereas the 3D model well corresponds to the observation. Using a 2D model (the shallow-water model), Hong and Yoon (1992) studied the sea-level variations in the Korea Strait (the Tsushima Strait) with the passing of a typhoon, and also obtained such a discrepancy between the model and the observation. They suggested that the discrepancy may be due to a vertical velocity shear and/or a baroclinic effect which can not be represented in 2D models. Such discrepancy has been also found in a recent numerical study by Minato (1998) who compared the elevation in Tosa Bay using a 2D model and a 3D model (Princeton ocean model: POM). These results suggest that the 3D models are more realistic for examining the response of coastal water to storm surges rather than the 2D models. The POM described by Blumberg and Mellor (1987) has been widely used by many coastal oceanographers because it is well documented and reproduces many of the observed features of the coastal and estuarine waters (Oey *et al.*, 1985; Galperin and Mellor, 1990a, 1990b).

The goal of this paper is to apply the POM to a typhoon characterised by Fujita (1952) for the air pressure and by Miyazaki *et al.* (1961) for the wind. In addition, the results between the 2D and 3D models are compared, and the bottom drag coefficient is discussed in terms of how to affect the current fields in the models.

NUMERICAL MODEL

Governing equations

The model used here is the Princeton ocean model (POM) described by Blumberg and Mellor (1987), and its configurations are almost the same to those of Hong and Choi (1997), except for atmospheric conditions, who studied tidal circulation in Deukryang Bay. It has free surface in sigma-coordinate (Fig. 1) and a split mode time step, and solves the traditional hydrodynamic equations for conservation of mass, momentum, temperature, and salinity coupled with the equation of state.

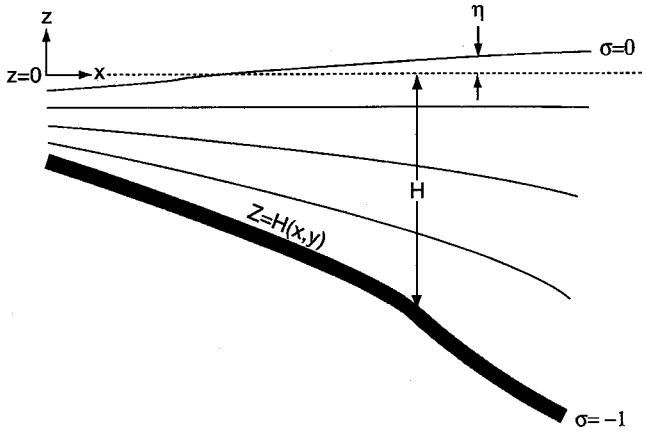

Fig. 1. The sigma coordinate system.

$$\frac{\partial u}{\partial x}+\frac{\partial v}{\partial y}+\frac{\partial w}{\partial z}=0 \tag{1}$$

$$\frac{\partial u}{\partial t}+u\frac{\partial u}{\partial x}+v\frac{\partial u}{\partial y}+w\frac{\partial u}{\partial z}-fv = -\rho_0^{-1}\frac{\partial p}{\partial x}+\frac{\partial}{\partial z}\left(K_M\frac{\partial u}{\partial z}\right)+F^x \tag{2}$$

$$\frac{\partial v}{\partial t}+u\frac{\partial v}{\partial x}+v\frac{\partial v}{\partial y}+w\frac{\partial v}{\partial z}+fu = -\rho_0^{-1}\frac{\partial p}{\partial y}+\frac{\partial}{\partial z}\left(K_M\frac{\partial v}{\partial z}\right)+F^y \tag{3}$$

$$\rho g=-\frac{\partial p}{\partial z} \tag{4}$$

$$\frac{\partial T}{\partial t}+u\frac{\partial T}{\partial x}+v\frac{\partial T}{\partial y}+w\frac{\partial T}{\partial z}=\frac{\partial}{\partial z}\left(K_H\frac{\partial T}{\partial z}\right)+F^T \tag{5}$$

$$\frac{\partial S}{\partial t}+u\frac{\partial S}{\partial x}+v\frac{\partial S}{\partial y}+w\frac{\partial S}{\partial z}=\frac{\partial}{\partial z}\left(K_H\frac{\partial S}{\partial z}\right)+F^S \tag{6}$$

$$\rho=\rho(T,S) \tag{7}$$

where u, v, and w are the velocity components in the x, y, and z directions, respectively, p the pressure including the atmospheric pressure by typhoon, T the temperature, S the salinity, ρ *in situ* density, ρ_0 (=constant) the reference density, f the Coriolis parameter, g the gravitational acceleration, K_M the vertical eddy viscosity, K_H the vertical eddy diffusivity, $F^{(x,\,y)}$ the horizontal eddy friction terms, and $F^{(T,\,S)}$ the horizontal eddy diffusion terms. The model assumes the Boussinesq and hydrostatic approximations and uses the Knudsen's equation to solve Equation 7. The K_M, K_H are determined by Mellor and Yamada level 2.5 turbulence closure model (Galperin *et al.*, 1988). The horizontal friction and diffusion terms are given by the Laplacian forms with the coefficients A_M and A_H given by Smagorinsky nonlinear viscosity. The model first transforms Equations 1—6 into σ coordinate system defined by $\sigma=(z-\eta)/(H+\eta)$, where η and H are the surface elevation and the water depth, respectively. The bottom drag coefficient (γ) is given as

$$\gamma=\mathrm{MAX}\left[\frac{k^2}{[\ln(1+\sigma_{kb-1})H/z_o]^2},\ 0.0025\right]$$

where $k=0.4$ is the von Karman constant and z_o the roughness parameter. As the depth deepens, $(1+\sigma_{kb-1})H/z_o$ becomes large and γ approaches to the constant (=0.0025). In the case that the region is shallow with a depth of a few meters, γ becomes very large and the current is rapidly damped. Bottom stress terms including γ in the model are derived by matching the numerical solution to the "law of the wall", and numerically, they are applied to the first grid points nearest the bottom (Mellor, 1996). For convenience, we here use the vertical velocity in the sigma coordinate ($w(\sigma)$), to discuss upwelling (or downwelling) phenomenon. Further details of the model are given by Blumberg and Mellor (1987).

Figure 2 depicts the topography of Deukryang Bay: the contours are generally parallel to the coastline of the bay. The bay is shallow in the western side and deep in the eastern side. This topography will influence the circulation pattern and distribution of sea water properties in the bay. The normal components of velocity at the coastal boundary are chosen to be zero. At open boundary, the normal components of the external-mode velocity are calculated from linearized momentum equation. The internal-mode velocity is given by the radiation condition of Orlanski (1976). The tangential components of both external- and internal-mode velocities are subject to free-slip condition, $\partial\bar{u}/\partial y=\partial u/\partial y=0$. The same condition is also given for temperature and salinity. Initial temperature condition is horizontally homogeneous and the values exponentially decrease from 28°C in the surface. Salinity distribution, on the other hand, is assumed to be equal everywhere to 34.50‰ and is used as a check of the finite difference technique on the conservation properties. Initial sea level and velocities are set to be zero, $u=v=\eta=0$. For simplicity, the heat flux through the open boundary is set constant; vertical temperature distribution is the same as the initial condition; the horizontal heat flux is given as that of Mellor (1996).

The horizontal grid is fixed to 1 km in both x and

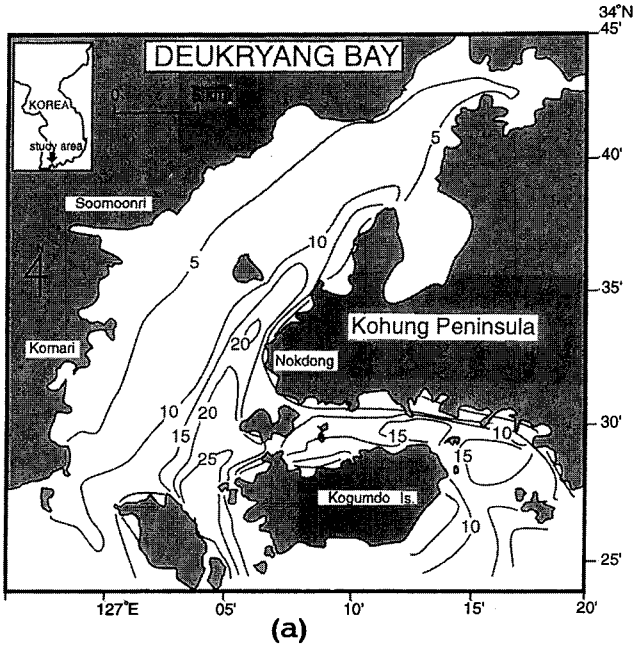

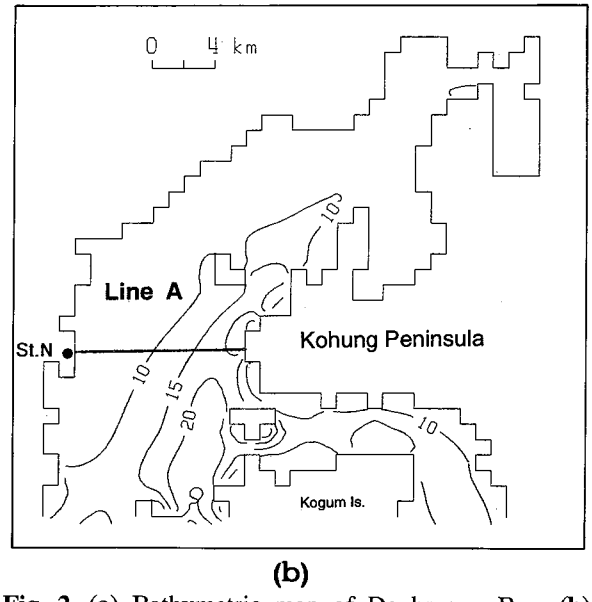

Fig. 2. (a) Bathymetric map of Deukryang Bay. (b) The model bathymetric map. Depths are in meters. Along Line A vertical sections of variables are shown and a comparison of elevations between the 2D and 3D models is given at St. N.

y directions. The model has 10 vertical levels with irregular vertical spacing in σ space as listed in Table 1. Refer to Hong and Choi (1997) for the details of the model.

Atmospheric conditions

The atmospheric condition in the model consists

Table 1. Vertical σ coordinate distribution

Level	σ'[1]	σ[2]	$\Delta\sigma$[3]
1	0.000		
		−0.010	0.021
2	−0.021		
		−0.029	0.021
3	−0.042		
		−0.059	0.042
4	−0.083		
		−0.118	0.083
5	−0.167		
		−0.236	0.167
6	−0.333		
		−0.417	0.167
7	−0.500		
		−0.583	0.167
8	−0.667		
		−0.764	0.167
9	−0.833		
		−0.917	0.167
10	−1.000		

[1] The depth at which turbulence quantities and the vertical velocity are located.
[2] The depth at which horizontal velocity, temperature, salinity, and density are defined.
[3] The grid spacing.

of the air pressure and the wind. The air pressure $P(x, y)$ at (x, y), originating from the center of a typhoon, is given by Fujita (1952);

$$P(x, y)=P_\infty-\delta P/\sqrt{1+(r/r_0)^2}$$

where P_∞ is the ambient pressure (theoretically at infinite radius; however, practically the value of the first anticyclonically curved isobar; Holland, 1980), δP a depression of the air pressure at the center of the typhoon, r the radius from the center of the typhoon, r_0 a distance at which the depression of the air pressure becomes $\delta P/\sqrt{2}$ having the maximum gradient wind (*i.e.*, the radius of the typhoon's core).

The wind distribution (W) given by Miyazaki *et al.* (1961) is obtained by the summation of the gradient wind (W_g) and the wind (W_b) which is proportional to the moving speed of the typhoon:

$$W=C_g W_g(r)+C_b W_b E^{-\alpha r}$$

where C_g (=0.8) and C_b (=0.5) are parameters for fitting to the observation, α a coefficient for exponentially decreased amount of W_b from the center of the typhoon. The gradient wind (W_g) is given by

$$W_g=\frac{rf}{2}\left(-1+\sqrt{1+\frac{4}{\rho_a r f^2}\frac{\partial P}{\partial r}}\right)$$

where ρ_a is the atmospheric density.

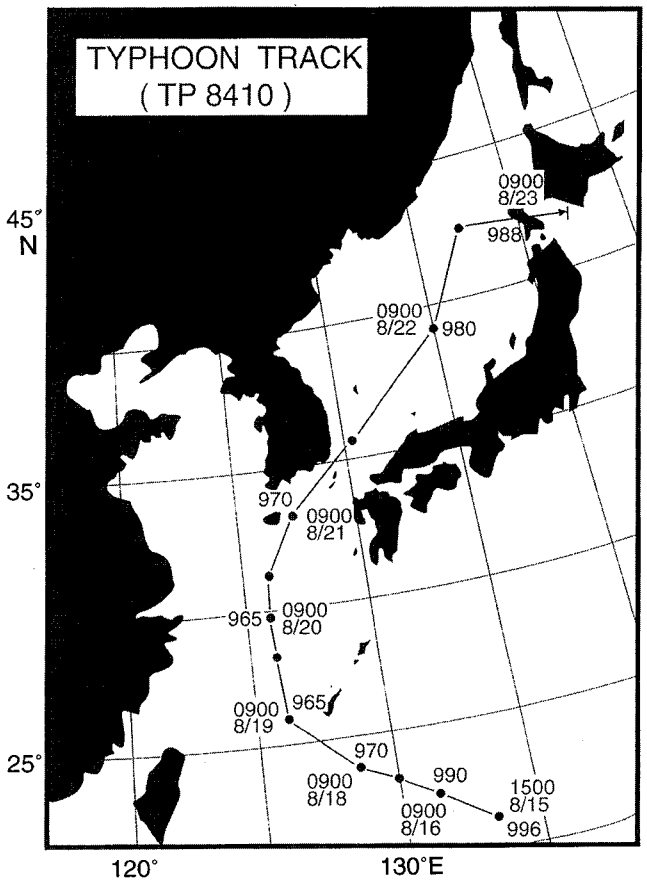

Fig. 3. The track of typhoon TP8410. Filled circle (●) represents the central position, and the numerals give the central pressures and the arrival time for each location.

The wind stresses (τ^x, τ^y) are calculated by

$$(\tau^x,\ \tau^y) = \rho_a C_d W(w_x,\ w_y)$$

where C_d ($=2.6\times10^{-3}$) is the drag coefficient of the wind, w_x and w_y are the components of W in x and y directions, respectively.

For implement of the model, the typhoon TP8410 (Fig. 3) tuned up by Hong (1996) was used for this study. The details concerned with setting of the model typhoon are given in Hong and Yoon (1992).

The model ran for about four days: from 00:00 local time August 20th, 1984 (hereafter 20:0000) to 24:0000. The run-time corresponds to the period of the typhoon being roughly located at the northeast of Taiwan until being changed to a weak cyclone in the Okhotsk Sea (see Fig. 3).

RESULTS

Response of Deukryang Bay to typhoon TP8410

We present the results at 21:0300 and 21:1800 because they well represent the main features of the seawater response in the whole period of the passing of the typhoon.

Figure 4 shows the wind vector (Fig. 4a) and the seawater elevation (Fig. 4b) at 21:0300 as well as the velocities (Figs. 4c and 4d), temperatures (Figs. 4e and 4f) and vertical velocities (Figs. 4g and 4h) in the upper and the lower layers. The typhoon is about 250 km south of Deukryang Bay, and its central pressure is 965 hpa. The sea water has been piled up westward due to Ekman transport (Fig. 4c) accompanied by the northeasterly wind (Fig. 4a) which has continued to blow almost in the same direction from its early stage. The coastal jet also has been well developed in the upper layer of the west side of the bay. The current field in the upper layer is decided nearly by the wind field. In the lower layer (Fig. 4d), however, the state becomes different. The outward current in the west side of the bay is rapidly damped due to its shallow depth (see Fig. 2), whereas the inward current begins to develope in the east side of the bay as a complemented flow to compensate the outward water mass. It is interesting that the current direction was opposed to the wind direction. Temperature field in the surface has been well mixed due to the strong surface current (Fig. 4e) but in the lower layer, cold-water mass appears in the east side of the bay forming horizontal contrast (Fig. 4f). Also in the surface temperature field we can find several cold-water zones around Kohung Peninsula. In Figs. 4g and 4h, the vertical velocity fields reveal that they are caused by the coastal upwelling and downwelling accompanied by the wind. Vertical sections of the temperature (Fig. 5a) and vertical velocity (Fig. 5b) along Line A (see Fig. 2 for location) show that the strong upwelling (blank zone in Fig. 5b) develops in the east side (Nokdong) of Deukryang Bay, transporting the cold water in the bottom to the surface, while the downwelling broadly occurs in the west side of the bay. In the model, mean upwelling velocity is about 0.03 cm/s. This value corresponds to about 26 m/day, implying that there should happen an overturn of sea water in Deukryang Bay with the passing of typhoons.

At 21:1800 when the typhoon is located around the Korea Strait, the direction of the wind in the bay has been changed to be northwesterly (Fig. 6a). This state is basically opposite to the one of the northeasterly wind in Fig. 4. The sea water is gradually

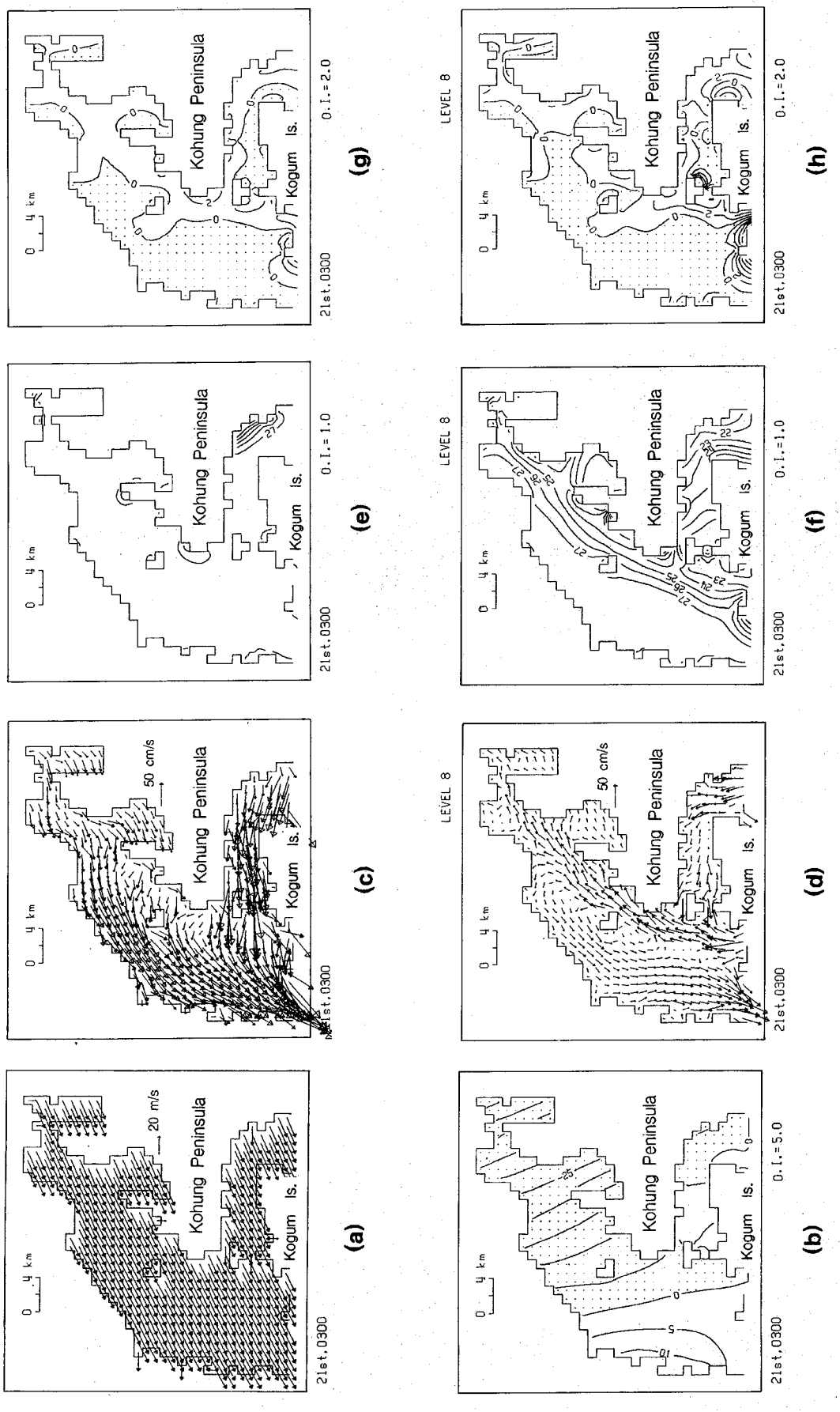

Fig. 4. (**a**) Wind vector (m/s), (**b**) seawater elevation (cm). The velocity (cm/s) (**c**)(**d**), the temperature (°C) (**e**)(**f**), and the vertical velocity ($\times 10^{-2}$ cm/s) (**g**)(**h**) in the upper and in the lower layers at 21:0300, respectively. The blank zones represent the negative values.

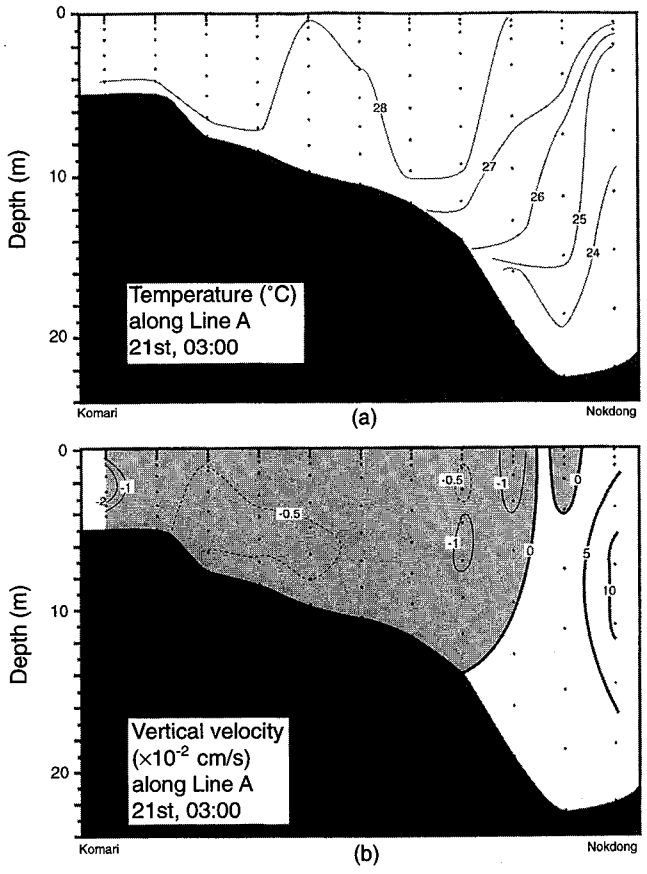

Fig. 5. Vertical sections of temperature (**a**) and vertical velocity (**b**) along Line A (see Fig. 2 for location) at 21: 0300. The stippled zone represents downwelling part.

piled up to the eastern side of the bay accompanied by the northwesterly wind (Fig. 6b), and the surface current has been changed to be south- or southeastward (Fig. 6c). In the lower layer, the northward longshore current still flows along the eastern coast and the current field persists the anticlockwise circulation (Fig. 6d). The surface temperature field (Fig. 6e) still has been well mixed, however, temperature in the east side (Fig. 6f) becomes slowly warmer due to the downwelling (Figs. 6g and 6h). This is more clearly shown in the vertical sections of temperature (Fig. 7a) and the vertical velocity (Fig. 7b) along Line A.

During the whole period of the passing of the typhoon, the vertical velocity shear in the bay has been very dominant, and baroclinicity of the flow also has been found. An example is given in Fig. 8 that shows vertical sections of north-south components of the velocity along Line A. Regardless of the change of the wind direction, strong velocity shear in the vertical direction develops in the whole period, and the baroclinicity of velocity is also dominant.

Comparison between 2D and 3D models

2D calculation can be done by the option of POM under the same condition of the parameters in 3D calculation except excluding the calculation of baroclinic components. It is formulated by vertically integrated Equations 1—3.

Figure 9 shows the elevations and the velocity fields in the 2D calculation at 21:0300 (Fig. 9a) and at 21:1800 (Fig. 9b). Distribution of the elevations is very similar to ones in the 3D model (see Fig. 4b and Fig. 6b), however, the amplitudes are generally smaller than the ones in the 3D model. Time series of the elevations (Fig. 10) at St. N (see Fig. 2 for location) show the differences of the amplitudes between the 2D and the 3D models. Their patterns are very similar, but the amplitude in the 3D model is larger than that in the 2D model, especially in the period of stronger northeasterly wind (refer to time series of the wind in Fig. 10). It means that the elevation in the 3D model has been more excited by the strong surface current (Fig. 4c). The velocity fields (Fig. 9) in the 2D model have been much reduced than the ones in the 3D model due to depth-averaged velocity without considering the vertical velocity shear and the baroclinicity of the velocity. In other word, when we consider that the effect of the typhoon is largely confined within several hundred meters in depth, the two-dimensional flow has been underestimated for the elevation due to averaging velocity in depth, whereas the three-dimensional flow has well represented surface current field for the elevation.

Dependance of the bottom friction on the depth is extremely natural; the shallower the depth, the stronger the bottom friction, and vice versa. Nevertheless, the bottom friction (the bottom drag coefficient) has been often regarded as a constant. In order to investigate the dependance of the bottom drag coefficient on the depth, additional experiments in the 2D and 3D models have been carried out under the same conditions except being a constant $\gamma\,(=0.0025)$ independent of the depth. An example in the velocity fields obtained from the experiments is given in Fig. 11. The velocity field in the 2D model at 21:0300 (Fig. 11a) has been remarkably increased due to weakness of the bottom friction effect (compare to Fig. 9a, here γ being

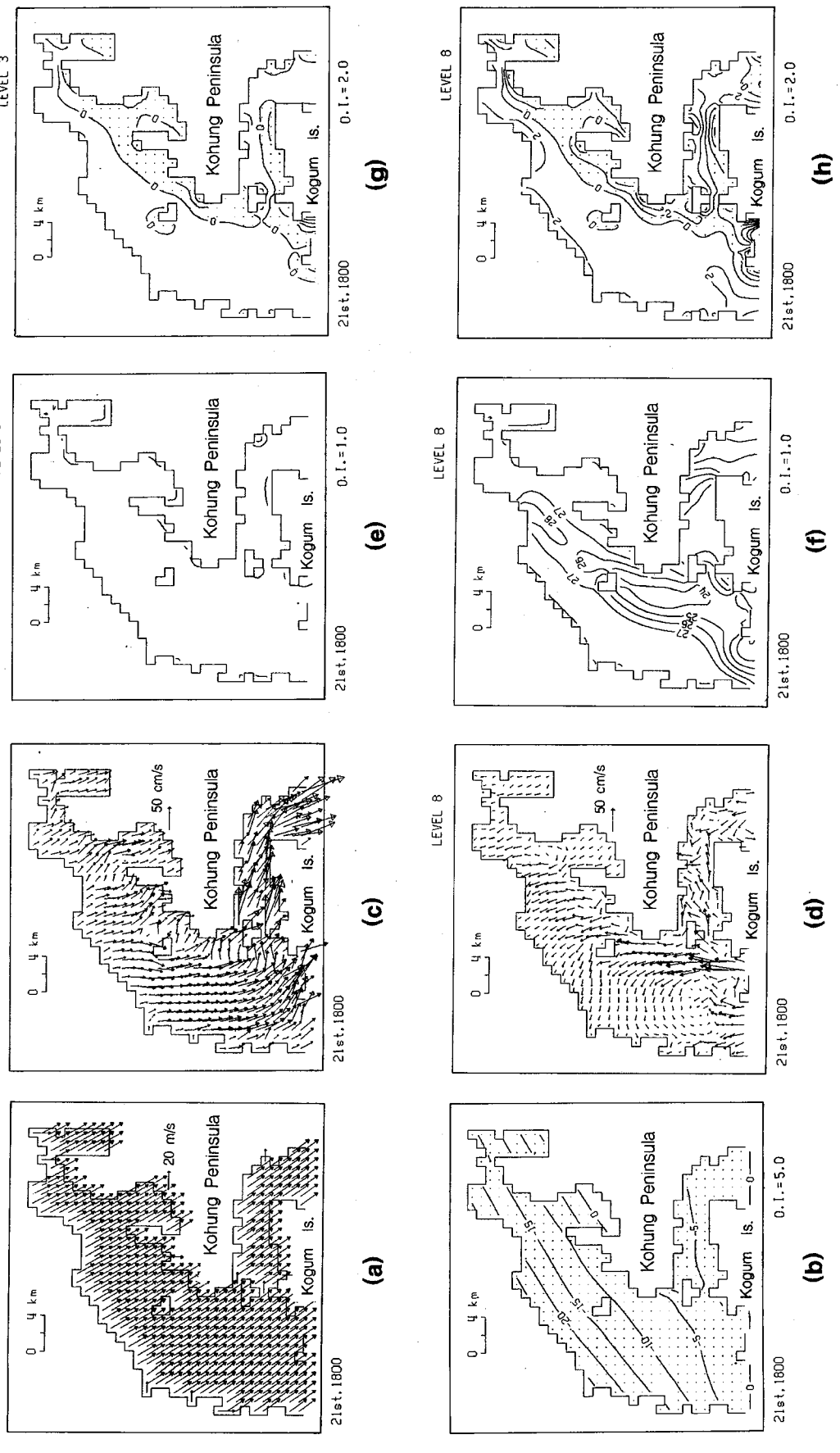

Fig. 6. Same as Fig. 4 but for at 21:1800.

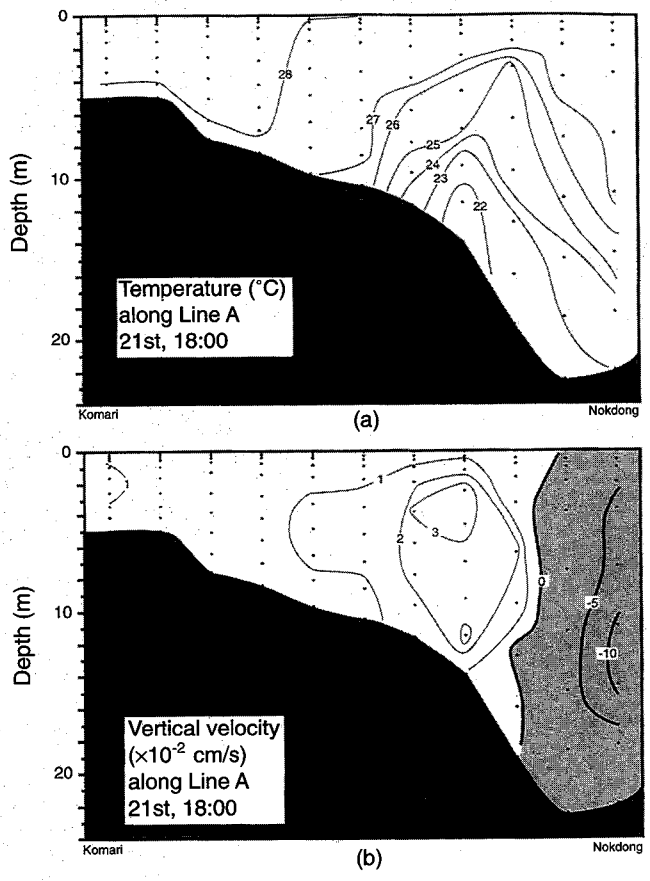

Fig. 7. Same as Fig. 5 but for at 21:1800.

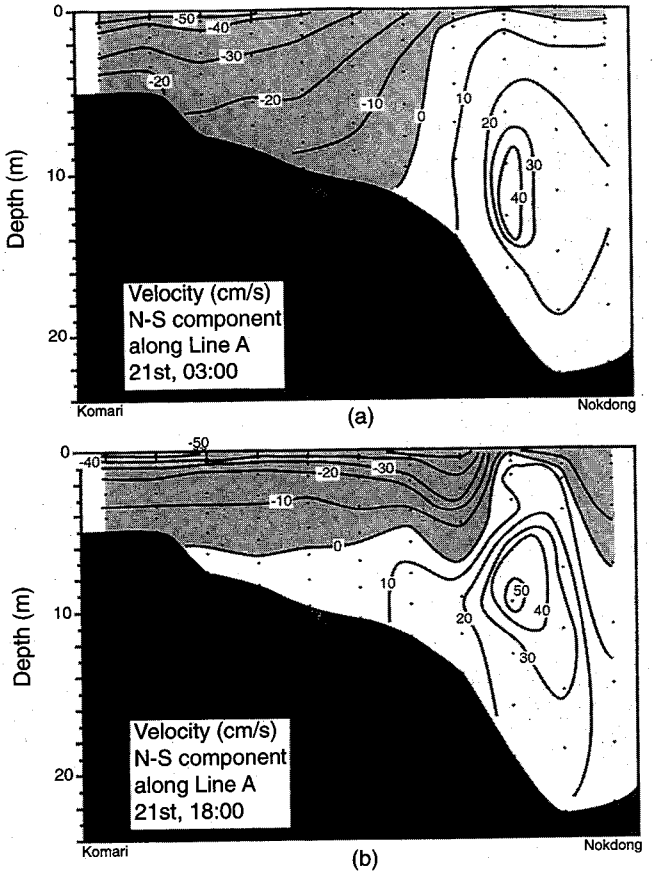

Fig. 8. The north-south component of current velocity (cm/s) along Line A at 21:0300 (**a**) and 21:1800 (**b**). The stippled zones represent the southward current.

dependent on depth). The elevation has also been increased (not presented here). In the 3D model the velocity field has also been increased, and in the lower layer (Fig. 11c) it tends more to have been increased. These results show that numerical results may be largely changed according to how to set γ, and that setting a constant γ is likely to overestimate the current field, particularly in a shallow bay such as Deukryang Bay. From these results it is postulated that bottom drag coefficient conventionally used for the flow field in 2D models is overestimating the computed current field.

DISCUSSION AND CONCLUSIONS

The Princeton ocean model (POM) is used to examine the response of sea water in Deukryang Bay to a typhoon. The results are (1) the model has well reproduced some features in the wind-driven dynamics, such as development of the coastal jet and upwelling (or downwelling) with the passing of a typhoon. (2) The model indicates that overturning of bay water occurs due to upwelling (or downwelling) generated by typhoon. (3) Regardless of the change of the wind direction, strong velocity shear in the vertical direction develops in the whole period of the typhoon and the baroclinicity of velocity forms. (4) Comparison of the results between the 2D and 3D models reveals that the 2D model may underestimate the current field in relation to reproducing the vertical velocity shear and the baroclinicity of velocity. (5) The model shows that numerical results may be significantly changed according to how to set bottom drag coefficient (γ), especially in a shallow bay like Deukryang Bay.

The model is, however, not verified by the observation in Deukryang Bay since there are no real-time data during the passing of typhoons. This must be certainly complemented in the future. Nevertheless, the results are easily understandable, and give us several meaningful insights into the storm surge dynamics. For example, it shows that an overturn of sea water in a shallow bay may occur

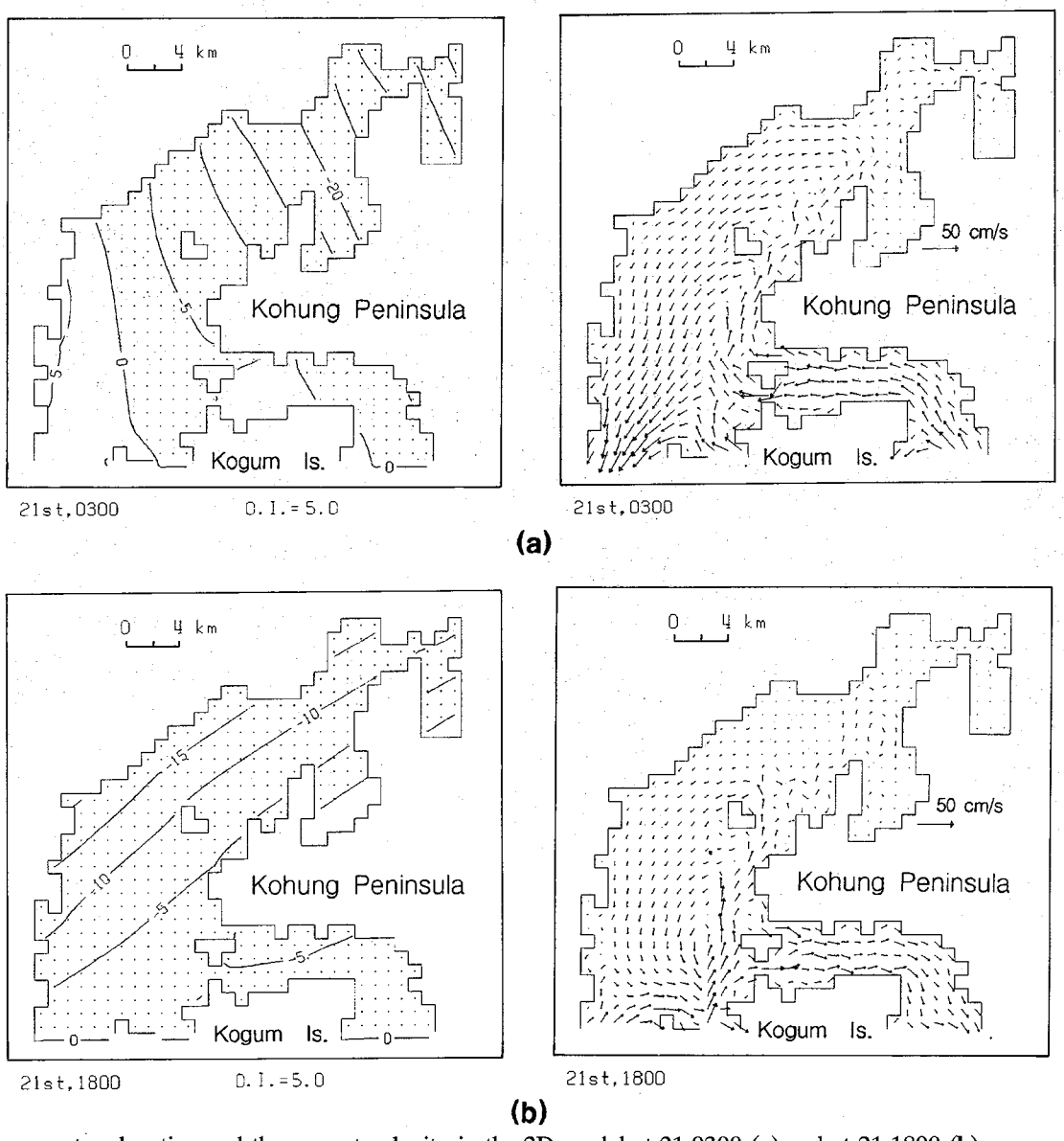

Fig. 9. The seawater elevation and the current velocity in the 2D model at 21:0300 (**a**) and at 21:1800 (**b**).

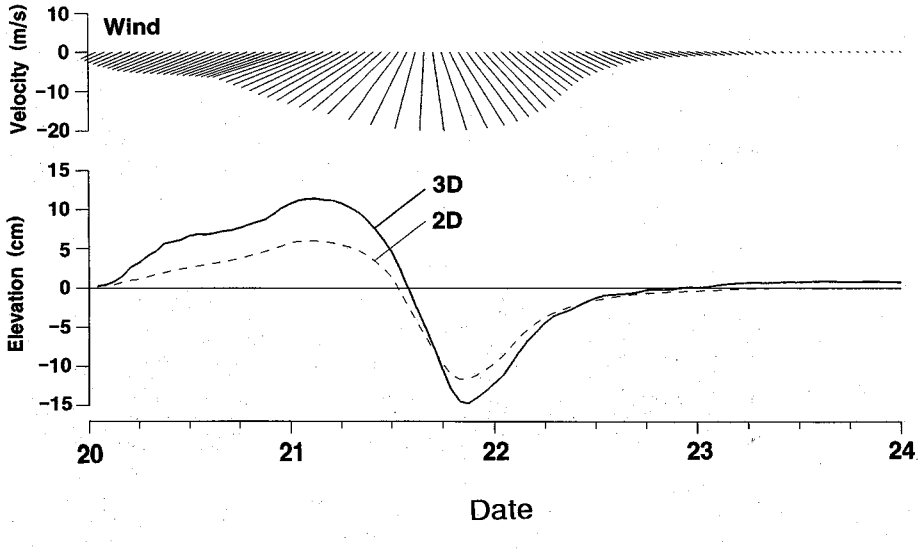

Fig. 10. Time series of the elevations in the 2D and 3D models at St. N (see Fig. 2 for location). The wind variation is given in the upper panel.

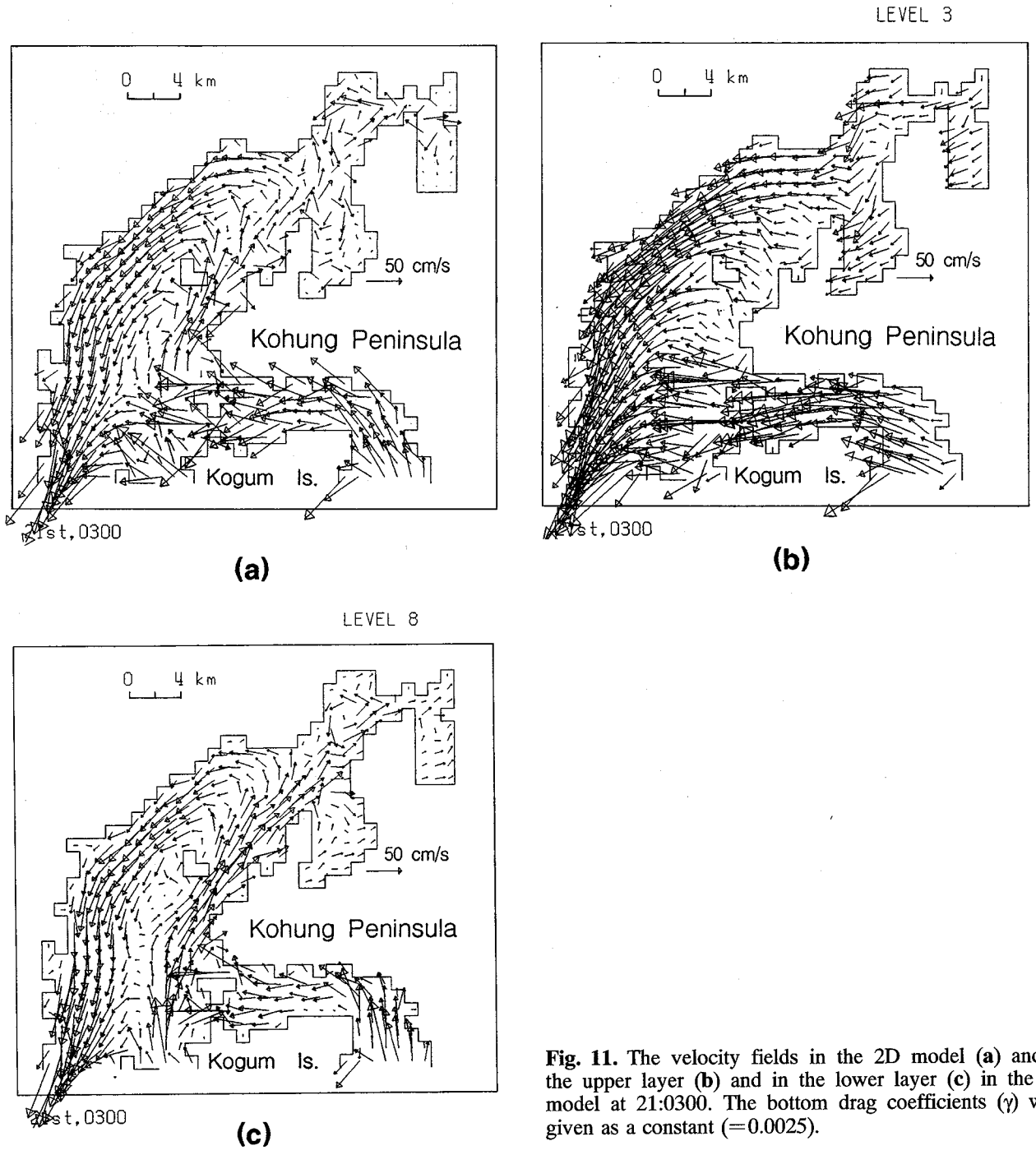

Fig. 11. The velocity fields in the 2D model (**a**) and in the upper layer (**b**) and in the lower layer (**c**) in the 3D model at 21:0300. The bottom drag coefficients (γ) were given as a constant ($=0.0025$).

due to upwelling and downwelling (see Figs. 4g, 4h, 6g and 6h) within several days during the passing of typhoons. We estimated upwelling velocity to be about 26 m/day based on vertical velocity in the sigma coordinate, $w(\sigma)$ of which the direction is normal to the sigma level. However, the values should be corrected by real vertical velocity, $w(z)$, in the gravity direction, since $w(\sigma)$ normal to the slope can involve horizontal velocity components (Mellor, 1996). Nevertheless, there would be little problem in discussing at least the upwelling phenomenon itself. The vertical velocity shear (*e.g.* Fig. 8) was very significant in the whole period of the typhoon, and then the baroclinicity in velocity field developed found. This exhibits that a depth-average model may be absolutely inadequate to represent the realistic velocity field, especially in the shallow bay. As already pointed out by several

authors (*e.g.* Hearn *et al.*, 1990; Minato, 1998), the discrepancy of the sea surface elevations between the 2D and 3D models may be related to limit of the 2D model which is inadequate to represent the velocity shear and the baroclinicity.

The bottom friction effect may also cause other problems in the 2D model, especially in the shallow region. In the case of constant γ, the velocity field has been remarkably increased than in the case of the depth-depended γ (see Figs. 9 and 11). Since bottom friction is basically dependent on the depth, the 3D model with depth-depended γ would be more plausible for examining the storm surge problem, although the results in the 3D model here were not validated by the observation.

ACKNOWLEDGMENTS

The author wishes to thank the two anonymous referees for their valuable comments and carefully reading the manuscript. He also wishes to acknowledge the financial support of the Korea Research Foundation in the program year of 1997. This study was also supported in part by the Korea Science and Engineering Foundation through the Research Center for Ocean Industrial Development of Pukyong National University.

REFERENCES

Blumberg, A.F. and G.L. Mellor, 1987. A description of a three dimensional coastal ocean circulation model. Three Dimensional Coastal Ocean Models; Coastal Estuarine Science (4th edn.), edited by Heap, N.S., American Geophysical Union, Washington DC, pp. 1–16.

Fujita, T., 1952. Pressure distribution within typhoon. *Geophys. Mag.*, **23**: 37–451.

Galperin, B. and G.L. Mellor, 1990a. A time-dependent, three-dimensional model of the Delaware Bay and River. Part 1. Description of the model and tidal analysis. *Est. Coast. Shelf Sci.*, **31**: 231–253.

Galperin, B. and G.L. Mellor, 1990b. A time-dependent, three-dimensional model of the Delaware Bay and River. Part 2. Three dimensional flow fields and residual circulation. *Est. Coast. Shelf Sci.*, **31**: 255–281.

Galperin, B., L.H. Kantha, S. Hassid and A. Rosati, 1988. A quasi-equilibrium turbulent energy model for geophysical flows. *J. Atmos. Sci.*, **45**: 55–62.

Hearn, C.J. and P.E. Holloway, 1990. A three-dimensional barotropic model of the response of the Australian North West Shelf to tropical cyclones. *J. Phys. Oceanogr.*, **20**: 60–80.

Heap, N.S., 1969. A two-dimensional numerical sea model. *Phil. Trans. R. Soc. Lond.*, **A265**: 93–137.

Holland, G.J., 1980. An analytical model of the wind and pressure profiles in hurricanes. *Mon. Wea. Rev.*, **108**: 1212–1218.

Hong, C.H., 1996. Sea level response in the Korea Strait to typhoons. *J. Korean Soc. Oceanogr.*, **31**: 107–116.

Hong, C.H. and Y.K. Choi, 1997. The response of temperature and velocity fields to M2 tide in the Deukryang Bay in the southern sea of Korea. *J. Korean Fish. Soc.*, **30**: 667–678.

Hong, C.H. and J.H. Yoon, 1992. The effect of typhoon on the coastal sea level variations in the Tsushima Straits. *J. Oceanogr. Soc. Japan* (*Umino Kenkyu*), **1**: 225–249. (in Japanese).

Konishi, T., 1989. Numerical forecast of storm surges on real time basis. *Oceanogr. Mag.*, **39**: 21–42.

Mellor, G., 1996. Users Guide for a Three-Dimensional, Primitive Equation, Numerical Ocean Model. Atmospheric and Oceanic Sciences Program (Princeton University), Princeton, 39 pp.

Minato, S., 1998. Storm surge simulation using POM and a revisitation of dynamics of sea surface elevation short-term variation. *Meteorol. Geophys.*, **48**: 79–88.

Miyazaki, M., T. Ueno and S. Unoki, 1961. Theoretical investigation of typhoons surges along the Japanese coast. *Oceanogr. Mag.*, **13**: 5–75.

Oey, L.Y., G.L. Mellor and R.I. Hires, 1985. A three-dimensional simulation of the Hudson Raritan estuary. Part I. Description of the model and model simulations. *J. Phys. Oceanogr.*, **15**: 1676–1692.

Orlanski, I., 1976. A simple boundary condition for unbounded hyperbolic flows. *J. Comp. Phys.*, **21**: 251–269.

Oh, I.S. and S.I. Kim, 1990. Numerical simulations of the storm surges in the seas around Korea. *J. Oceanol. Soc. Korea*, **25**: 161–181.

Platzman, G.W., 1963. The Dynamical Prediction of Wind Tides on Lake Erie. American Meteorological Society, Monograph, Vol. 26, 44 pp.

Manuscript received April 6, 1998
Revision accepted July 22, 1998